Energy and Helicity Analysis in Two-Fluid Modeling

J. P. Sauppe, C. R. Sovinec

University of Wisconsin-Madison

NIMROD Team Meeting
March 14, 2015

Outline

Review of Flow Results in NIMROD

Momentum Analysis

Magnetic Helicity and Variational Theories

Energy and Helicity Analysis

Unresolved Issues

Conclusions

Outline

Review of Flow Results in NIMROD

Momentum Analysis

Magnetic Helicity and Variational Theories

Energy and Helicity Analysis

Unresolved Issues

Conclusions

Intrinsic plasma flow is observed in MST and appears highly coupled with the relaxation dynamics.

- Significant parallel flow with strong shear between sawteeth
- Parallel flow flattens at crash suggesting **strong coupling between the flow and current relaxation**

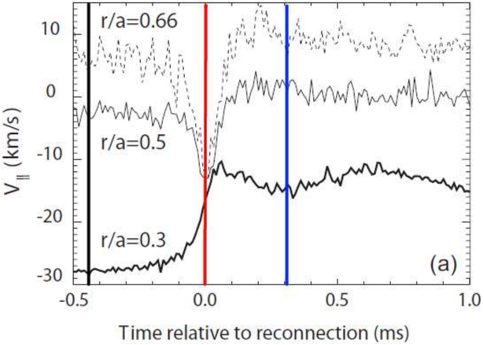

Kuritsyn et. al. PoP **16** 055903 (2009)

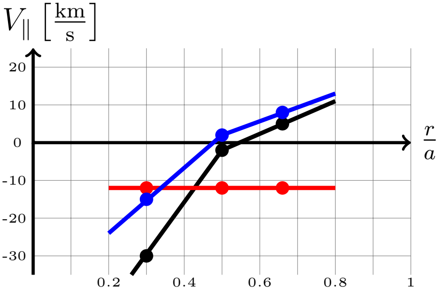

- In the core, $dV_{\|}/dt > 0$ at the event

NIMROD, a 3D extended MHD code that includes two-fluid physics, is used to study relaxation dynamics.

- The model includes two-fluid physics and first order FLR corrections:

$$\frac{\partial n}{\partial t} = -\nabla \cdot (n\mathbf{v}) + D_n \nabla^2 n$$

$$m_i n \left(\frac{\partial \mathbf{v}}{\partial t} + \mathbf{v} \cdot \nabla \mathbf{v} \right) = \mathbf{J} \times \mathbf{B} - \nabla (nT) - \nabla \cdot \underline{\mathbf{\Pi}}_{iso} - \underline{\nabla \cdot \underline{\mathbf{\Pi}}_{gv}}$$

$$\frac{n}{\Gamma - 1} \left(\frac{\partial T}{\partial t} + \mathbf{v} \cdot \nabla T \right) = -nT (\nabla \cdot \mathbf{v}) + \nabla \cdot (\chi n \nabla T)$$

$$\frac{\partial \mathbf{B}}{\partial t} = -\nabla \times \left[-\mathbf{v} \times \mathbf{B} + \underline{\frac{1}{ne} (\mathbf{J} \times \mathbf{B} - \nabla p_e)} + \eta \mathbf{J} + \underline{\frac{m_e}{ne^2} \frac{\partial \mathbf{J}}{\partial t}} \right]$$

$$\underline{\mathbf{\Pi}}_{iso} = \nu m_i n \underline{\mathbf{W}} \qquad \underline{\mathbf{W}} = \nabla \mathbf{v} + \nabla \mathbf{v}^T - \frac{2}{3} (\nabla \cdot \mathbf{v}) \underline{\mathbf{I}}$$

$$\underline{\mathbf{\Pi}}_{gv} = \frac{m_i p_i}{4eB} \left[\hat{\mathbf{b}} \times \underline{\mathbf{W}} \cdot \left(\underline{\mathbf{I}} + 3\hat{\mathbf{b}}\hat{\mathbf{b}} \right) - \left(\underline{\mathbf{I}} + 3\hat{\mathbf{b}}\hat{\mathbf{b}} \right) \cdot \underline{\mathbf{W}} \times \hat{\mathbf{b}} \right]$$

- Simulation Parameters:

$S = 20,000 \qquad P_m = \nu/\eta = 1 \qquad \chi/\eta = 0.1 = D_n/\eta \qquad \tau_A = 1$

$\beta = 0.1 \qquad d_i/a = 0.173 \qquad \rho_s/a = 0.05 \qquad m_e/m_i = 2.72 \cdot 10^{-3}$

- **MHD** all not underlined, **Cold Ion** + red, **Warm Ion** + red & blue

Two-fluid simulations have shown significant changes in plasma flow at the relaxation event.

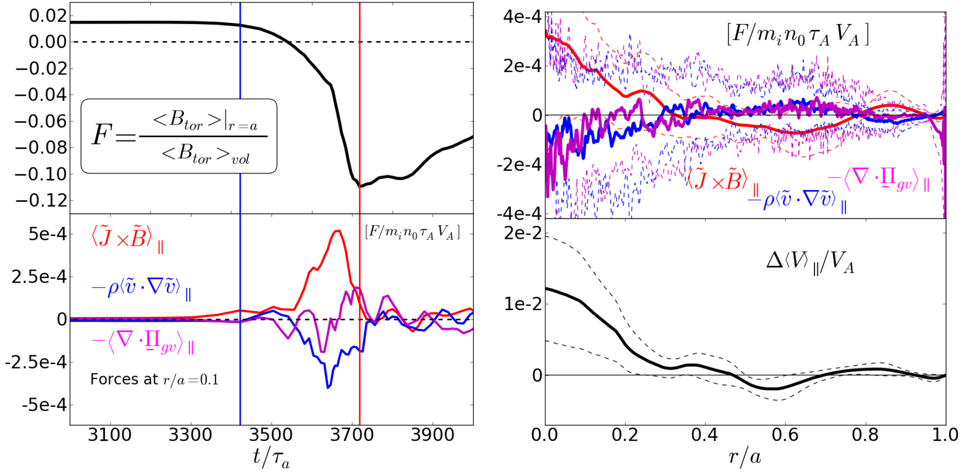

- With $E_m >> E_k$ the magnetics should decide the direction of flow changes
- Figure on left shows stresses at $r/a = 0.1$ with a rolling average in time
- Figure on right shows stresses at all r averaged over the relaxation event

Significant changes in axial and angular momentum are observed for cases with a two-fluid Ohm's law.

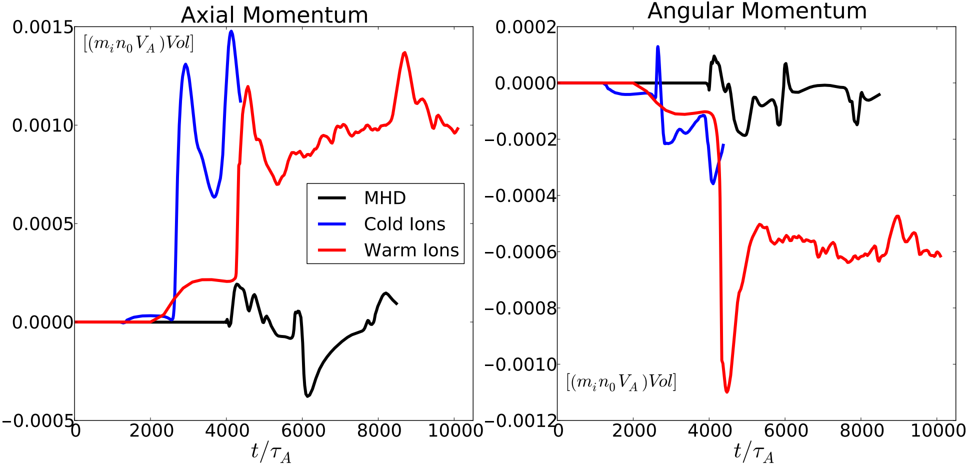

- Axial momentum changes significantly for both warm and cold ions
- Angular momentum only changes significantly for warm ions

Outline

NIMROD system does not conserve momentum exactly.

- The Lorentz force term only transports momentum, it does **not** impart net momentum to the plasma
- In the physical system, momentum is conserved up to viscous interaction with the wall
- The momentum evolution in the NIMROD system:

$$\frac{\partial \mathbf{P}}{\partial t} = \int \frac{\partial}{\partial t}\left(m_i n \mathbf{v}\right) d^3x = \int \left[m_i \mathbf{v} \frac{\partial n}{\partial t} + m_i n \frac{\partial \mathbf{v}}{\partial t}\right] d^3x$$
$$= \int \left\{-\boldsymbol{\nabla}\cdot\left(\underline{\underline{\boldsymbol{\Pi}}}_i - \underline{\underline{\boldsymbol{\Pi}}}_{i,\mathrm{eq}}\right) + \underline{m_i \mathbf{v} \boldsymbol{\nabla}\cdot\left[D_n \boldsymbol{\nabla}\left(n - n_{\mathrm{eq}}\right)\right]}\right\} d^3x$$
$$+ \int \left[\underline{m_i \mathbf{v} \boldsymbol{\nabla}\cdot\left(n_{\mathrm{eq}} \mathbf{v}_{\mathrm{eq}}\right)} + \underline{m_i n_{\mathrm{eq}} \mathbf{v}_{\mathrm{eq}} \cdot \boldsymbol{\nabla} \mathbf{v}_{\mathrm{eq}}}\right] d^3x$$

- In the numerical system, additional terms are present

$$\frac{\partial n}{\partial t} = -\boldsymbol{\nabla}\cdot\left(n\mathbf{v} - D_n \boldsymbol{\nabla} n\right) \quad \rightarrow \frac{\partial n}{\partial t} = -\boldsymbol{\nabla}\cdot\left(n\mathbf{v} - n_{\mathrm{eq}}\mathbf{v}_{\mathrm{eq}}\right) + \boldsymbol{\nabla}\cdot\left[D_n \boldsymbol{\nabla}\left(n - n_{\mathrm{eq}}\right)\right]$$

- Artifical density diffusion $\underline{D_n \boldsymbol{\nabla} n}$ term in the density equation
- Equilibrium terms in yellow result from NIMROD's assumption of force balance in equilibrium fields

Post-processing diagnostics construct each of the terms in the evolution equations for numerical simulations.

- NIMROD represents fields with $\mathcal{C}^0$ finite elements in the $R-Z$ plane and a Fourier series in ϕ
- Integration-by-parts is used to eliminate second derivatives:

$$\int 2T\boldsymbol{\nabla}\cdot\left(D_n\boldsymbol{\nabla}n\right)d^3x = \int\left[\boldsymbol{\nabla}\cdot\left(2TD_n\boldsymbol{\nabla}n\right)-\left(D_n\boldsymbol{\nabla}n\right)\cdot\boldsymbol{\nabla}\left(2T\right)\right]d^3x$$

$$\int \mathbf{v}\cdot\left(\boldsymbol{\nabla}\cdot\underline{\mathbf{\Pi}}\right)d^3x = \int\left[\boldsymbol{\nabla}\cdot\left(\underline{\mathbf{\Pi}}\cdot\mathbf{v}\right)-\underline{\mathbf{\Pi}}:\left(\boldsymbol{\nabla}\mathbf{v}\right)^T\right]d^3x$$

- Auxiliary fields are required for higher-order derivatives

$$\int \boldsymbol{\alpha}\cdot\left(\boldsymbol{\nabla}\cdot\underline{\mathbf{\Pi}}\right)d^3x = \int\left\{\boldsymbol{\nabla}\cdot\left[\underline{\mathbf{\Pi}}\cdot\boldsymbol{\alpha}\right]-\underline{\underline{\mathbf{\Pi}}:\left[\boldsymbol{\nabla}\boldsymbol{\alpha}\right]^T}\right\}d^3x \qquad \alpha = \boldsymbol{\nabla}\times\mathbf{v}$$

- Terms are constructed by transforming to real space and aliasing errors may be present for combinations of more than two fields

$$\int \frac{1}{ne}\left(\mathbf{J}\times\mathbf{B}\right)\cdot\boldsymbol{\nabla}\times\mathbf{v}\; d^3x$$

Cold ion momentum evolution is dominated by viscous interaction with the wall.

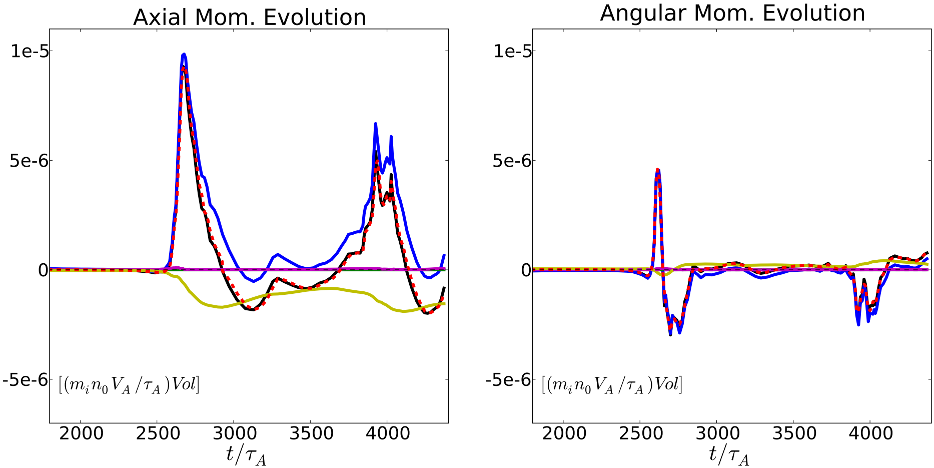

- Density diffusion term is negligible but not equilibrium pinch flow term

$$\frac{\partial \mathbf{P}}{\partial t} = \int \left\{ -\underline{\boldsymbol{\nabla}\cdot\left(\underline{\boldsymbol{\Pi}}_{iso} - \underline{\boldsymbol{\Pi}}_{iso,\mathrm{eq}}\right)} + \underline{m_i \mathbf{v} \boldsymbol{\nabla}\cdot\left[D_n \boldsymbol{\nabla}\left(n - n_{\mathrm{eq}}\right)\right]} + \underline{m_i \mathbf{v} \boldsymbol{\nabla}\cdot\left(n_{\mathrm{eq}} \mathbf{v}_{\mathrm{eq}}\right)} \right\} d^3x$$

Warm ion simulations show a careful balance between gyroviscosity and isotropic viscosity.

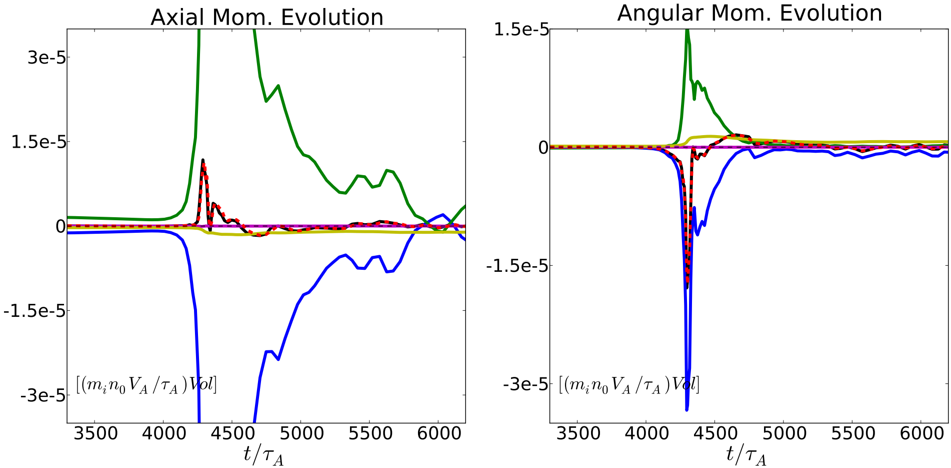

$$\frac{\partial \mathbf{P}}{\partial t} = \int \left\{ -\underline{\nabla \cdot \left(\underline{\mathbf{\Pi}}_{iso} - \underline{\mathbf{\Pi}}_{iso,\mathrm{eq}} \right)} - \underline{\nabla \cdot \left(\underline{\mathbf{\Pi}}_{gyr} - \underline{\mathbf{\Pi}}_{gyr,\mathrm{eq}} \right)} \right\} d^3x$$

$$+ \int \left[\underline{m_i \mathbf{v} \nabla \cdot \left[D_n \nabla \left(n - n_{\mathrm{eq}} \right) \right]} + \underline{m_i \mathbf{v} \nabla \cdot \left(n_{\mathrm{eq}} \mathbf{v}_{\mathrm{eq}} \right)} \right] d^3x$$

Outline

A variational theory based on selective decay of ideal invariants is used to predict the relaxed state.

- Taylor[1] recognized that the **magnetic helicity** ($\mathcal{K}$), a topological measure of the linkedness of magnetic field, is more robustly conserved than the magnetic energy in a resistive plasma

$$\mathcal{K} \equiv \int \mathbf{A} \cdot \mathbf{B} d^3x \qquad \frac{\partial \mathcal{K}}{\partial t} = \int \mathbf{E} \cdot \mathbf{B} d^3x \sim \int \frac{\eta}{\mu_0} \left[\sum_k k B_k^2 \right] d^3x$$

$$W_B \equiv \int \frac{\mathbf{B} \cdot \mathbf{B}}{2\mu_0} d^3x \qquad \frac{\partial W_B}{\partial t} = \int \frac{\mathbf{E} \cdot \mathbf{J}}{\mu_0} d^3x \sim \int \frac{\eta}{\mu_0} \left[\sum_k k^2 B_k^2 \right] d^3x$$

- Variational theory conserves magnetic helicity while minimizing energy

$$0 = \delta \left[W_B - \frac{\lambda}{2\mu_0} \mathcal{K} \right] = \int \frac{\delta \mathbf{A}}{\mu_0} \cdot \left[\nabla \times \mathbf{B} - \lambda \mathbf{B} \right] d^3x \quad \rightarrow \quad \nabla \times \mathbf{B} = \lambda \mathbf{B}$$

- Relaxed state is force-free ($\mathbf{J} \times \mathbf{B} = \mathbf{0}$) with λ a **global constant**
- The axisymmetric solution yields the Bessel function model (BFM)

$$B_z = B_0 J_0 (\lambda r) \qquad B_\theta = B_0 J_1 (\lambda r)$$

---

[1] Taylor, J. B. 1974. Relaxation of Toroidal Plasma and Generation of Reverse Magnetic Fields. *Physical Review Letters* **33**(19) 1139–1141

Plasma flow can be introduced into a variational formulation through the cross helicity.

- The **cross helicity** $\mathcal{X} \equiv \int \mathbf{v} \cdot \mathbf{B}\, d^3x$ is a measure of parallel flow[2]

$$\frac{\partial \mathcal{X}}{\partial t} = \int \left[\frac{1}{m_i n} \mathbf{F} \cdot \mathbf{B} - (\mathbf{E} + \mathbf{v} \times \mathbf{B}) \cdot \nabla \times \mathbf{v} \right] d^3x$$

- Invariant in **single-fluid ideal MHD** for: $\beta = 0$ <u>or</u> **barotropic** plasma

$$\frac{\mathbf{F} \cdot \mathbf{B}}{m_i n} = -\frac{\nabla p}{m_i n} \cdot \mathbf{B} = -\frac{1}{m_i} \nabla h \cdot \mathbf{B} = -\nabla \cdot \left(\frac{h\mathbf{B}}{m_i} \right) \qquad \frac{dh}{dn} \equiv \frac{1}{n} \frac{dp}{dn}$$

- No reason to expect the cross helicity is better conserved than energy

$$\frac{\partial \mathcal{X}}{\partial t} \approx \int -\eta \mathbf{J} \cdot \nabla \times \mathbf{v} \sim \int \eta \left[\sum_k k^2 v_k B_k \right] d^3x$$

- Variational principles that minimize energy while conserving magnetic helicity and cross helicity predict **field-aligned current and flow**

$$\delta \left[W_B + W_K - \frac{\lambda_0}{2\mu_0} \mathcal{K} - (m_i n)\, \lambda_1 \mathcal{X} \right] = 0 \rightarrow \begin{cases} \mathbf{v} = \lambda_1 \mathbf{B} \\ \nabla \times \mathbf{B} = \frac{\lambda_0}{1 - \mu_0 m_i n \lambda_1^2} \mathbf{B} \end{cases}$$

---

[2] Finn, J. M., T. J. Antonsen. 1983. Turbulent relaxation of compressible plasmas with flow. *Physics of Fluids* **26**(12) 3540–3552

An invariant hybrid helicity can be constructed if the Hall term is included in the generalized Ohm's law.[3]

- Hall physics in Ohm's law changes the cross helicity evolution

$$\frac{\partial \mathcal{X}}{\partial t} \sim \int -(\mathbf{E} + \mathbf{v} \times \mathbf{B}) \cdot \boldsymbol{\nabla} \times \mathbf{v} \; d^3x \quad \rightarrow \quad \int \frac{1}{ne} (\boldsymbol{\nabla} p_e - \mathbf{J} \times \mathbf{B}) \cdot \boldsymbol{\nabla} \times \mathbf{v} \; d^3x$$

- Introduce **kinetic helicity**

$$\mathcal{H} \equiv \int \mathbf{v} \cdot \boldsymbol{\nabla} \times \mathbf{v} \; d^3x \qquad \frac{\partial \mathcal{H}}{\partial t} = \int \frac{2}{m_i n} \mathbf{F} \cdot \boldsymbol{\nabla} \times \mathbf{v} \; d^3x$$

- The **hybrid helicity** is a weighted sum of $\mathcal{K}$, $\mathcal{X}$, and $\mathcal{H}$

$$H \equiv \mathcal{K} + 2 \left(\frac{m_i}{e} \right) \mathcal{X} + \left(\frac{m_i}{e} \right)^2 \mathcal{H}$$

- The hybrid helicity is conserved in **ideal Hall MHD** if $p_i = 0$ or the plasma is barotropic

$$\frac{\partial H}{\partial t} = \int -\frac{2}{ne} \boldsymbol{\nabla} p_i \cdot \left[\mathbf{B} + \left(\frac{m_i}{e} \right) \boldsymbol{\nabla} \times \mathbf{v} \right] \; d^3x$$

[3] Turner, L. 1986. Hall Effects on Magnetic Relaxation. *IEEE Transactions on Plasma Science* **PS-14**(6) 849–857

Outline

The magnetic helicity is more robustly conserved than the magnetic energy at the relaxation event.

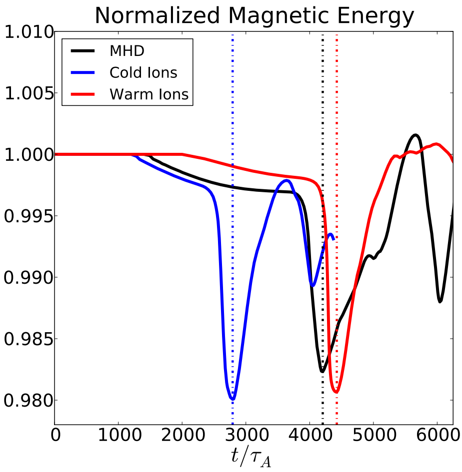

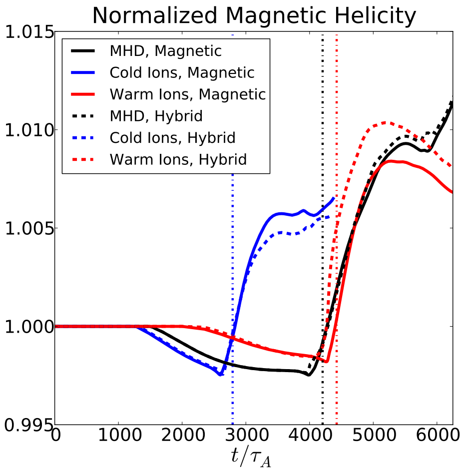

- Dashed vertical lines indicate the time of minimum magnetic energy
- The magnetic helicity has changed by only a small percentage while the energy has dropped by $\sim 2\%$
- The hybrid helicity is very nearly equal to the magnetic helicity

The equations we use do not conserve energy exactly.

- Magnetic energy with a two-fluid Ohm's law evolves as

$$\frac{\partial W_B}{\partial t} = -\int \frac{\mathbf{E}\times\mathbf{B}}{\mu_0}\cdot\hat{\mathbf{n}}dA + \int \left[\underline{\mathbf{v}\times\mathbf{B}\cdot\mathbf{J}} - \underline{\eta\mathbf{J}\cdot\mathbf{J}} + \underline{\tfrac{1}{ne}\mathbf{J}\cdot\nabla p_e}\right] d^3x$$

- The pinch flow provides a small injection of kinetic energy and the density diffusion provides an anomalous source/sink

$$\frac{\partial W_K}{\partial t} = \int \left[\underline{\mathbf{v}\cdot(\mathbf{J}\times\mathbf{B})} - \underline{\mathbf{v}\cdot\nabla p} - \underline{\mathbf{v}\cdot(\nabla\cdot\underline{\mathbf{\Pi}}_{iso})} - \underline{\mathbf{v}\cdot\left(\nabla\cdot\underline{\mathbf{\Pi}}_{gyr}\right)}\right] d^3x$$
$$- \int \left(\frac{1}{2}m_i n v^2\right)\mathbf{v}\cdot\hat{\mathbf{n}}dA + \int \left[\underline{\left(\tfrac{1}{2}m_i v^2\right)\nabla\cdot(D_n\nabla n)}\right] d^3x$$

- Single temperature modeling results in the $\underline{\mathbf{J}\cdot\nabla p_e}$ term in magnetic energy being unbalanced

$$\frac{\partial W_p}{\partial t} = \int \left[\frac{-\Gamma p\mathbf{v}}{\Gamma-1} - 2\mathbf{q}\right]\cdot\hat{\mathbf{n}}dA + \int \left[\underline{\mathbf{v}\cdot\nabla p} + \underline{\underline{\mathbf{\Pi}}_{iso} : (\nabla\mathbf{v})^T} + \underline{Q}\right] d^3x$$
$$+ \int \left[\underline{\tfrac{2T}{\Gamma-1}\nabla\cdot(D_n\nabla n)}\right] d^3x$$

- The $\frac{1}{ne}\mathbf{J}\cdot\nabla p_e$ term shows up in electron internal energy (from the $\mathbf{v}_e\cdot\nabla p_e$ term) if separate temperature modeling is used

Conservation of hybrid helicity depends on coupling.

- Magnetic helicity with a two-fluid Ohm's law evolves as

$$\frac{\partial \mathcal{K}}{\partial t} = \int \left[-2\eta \mathbf{J} \cdot \mathbf{B} + 2\mathbf{B} \cdot \left(\tfrac{1}{ne} \boldsymbol{\nabla} p_e \right) \right] d^3x$$

- The $\mathbf{B} \cdot \boldsymbol{\nabla} p_e$ from Hall physics couples this to cross helicity evolution

$$2\left(\frac{m_i}{e}\right)\frac{\partial \mathcal{X}}{\partial t} = \int \left[-2\left(\tfrac{m_i}{e}\right)\left(\tfrac{1}{ne}\right)(\mathbf{J}\times\mathbf{B})\cdot\boldsymbol{\nabla}\times\mathbf{v} + 2\left(\tfrac{m_i}{e}\right)\left(\tfrac{1}{ne}\right)(\boldsymbol{\nabla} p_e)\cdot\boldsymbol{\nabla}\times\mathbf{v} \right] d^3x$$
$$+ \int \left[-2\left(\tfrac{m_i}{e}\right)\eta \mathbf{J}\cdot\boldsymbol{\nabla}\times\mathbf{v} - 2\mathbf{B}\cdot\left(\tfrac{1}{ne}\boldsymbol{\nabla} p_e\right) - 2\mathbf{B}\cdot\left(\tfrac{1}{ne}\boldsymbol{\nabla} p_i\right) - 2\mathbf{B}\cdot\left(\tfrac{1}{ne}\boldsymbol{\nabla}\cdot\underline{\mathbf{\Pi}}_i\right) \right] d^3x$$

- The Hall terms in red and orange couple cross helicity and kinetic helicity

$$\left(\frac{m_i}{e}\right)^2 \frac{\partial \mathcal{H}}{\partial t} = \int \left[2\left(\tfrac{m_i}{e}\right)\left(\tfrac{1}{ne}\right)\mathbf{J}\times\mathbf{B}\cdot\boldsymbol{\nabla}\times\mathbf{v} - 2\left(\tfrac{m_i}{e}\right)\left(\tfrac{1}{ne}\right)\boldsymbol{\nabla} p_e\cdot\boldsymbol{\nabla}\times\mathbf{v} \right] d^3x$$
$$+ \int \left[-2\left(\tfrac{m_i}{e}\right)\left(\tfrac{1}{ne}\boldsymbol{\nabla} p_i\right)\cdot\boldsymbol{\nabla}\times\mathbf{v} - 2\left(\tfrac{m_i}{e}\right)\left(\tfrac{1}{ne}\boldsymbol{\nabla}\cdot\underline{\mathbf{\Pi}}_i\right)\cdot\boldsymbol{\nabla}\times\mathbf{v} \right] d^3x$$

- Terms in yellow vanish for either cold ions or barotropic ions
- Terms in purple vanish for an ideal plasma
- The isotropic viscosity piece of the stress in green also vanishes for an ideal plasma, **but not the gyroviscous part**

The constant loop voltage injects magnetic energy and helicity into the system.

- The magnetic energy evolves as

$$\frac{\partial W_B}{\partial t} = -\int \frac{\mathbf{E}\times\mathbf{B}}{\mu_0}\cdot\hat{\mathbf{n}}dA + \int\left[\mathbf{v}\times\mathbf{B}\cdot\mathbf{J} - \eta J^2 + \mathbf{J}\cdot\frac{1}{ne}\boldsymbol{\nabla}p_e\right]d^3x$$

- The only tangential electric field is the constant loop voltage, which balances the contributions from the equilibrium $\mathbf{E}_{\mathrm{eq}} = -\mathbf{v}_{\mathrm{eq}}\times\mathbf{B}_{\mathrm{eq}} + \eta\mathbf{J}_{\mathrm{eq}}$

$$\frac{\partial W_B}{\partial t} = \int\left[\underline{(\mathbf{v}\times\mathbf{B} - \mathbf{v}_{\mathrm{eq}}\times\mathbf{B}_{\mathrm{eq}})\cdot\mathbf{J}} - \underline{\eta\left(\mathbf{J}-\mathbf{J}_{\mathrm{eq}}\right)\cdot\mathbf{J}} + \underline{\mathbf{J}\cdot\tfrac{1}{ne}\boldsymbol{\nabla}p_e}\right]d^3x$$

- The relative magnetic helicity $\mathcal{K}_{rel} \equiv \int\left(\mathbf{A}-\mathbf{A}'\right)\cdot\left(\mathbf{B}+\mathbf{B}'\right)d^3x$ evolves as

$$\frac{\partial\mathcal{K}}{\partial t} = -2\int\left[\mathbf{E}\cdot\mathbf{B} - \mathbf{E}'\cdot\mathbf{B}'\right]d^3x = -2\int\left[\eta\mathbf{J}\cdot\mathbf{B} - \mathbf{B}\cdot\frac{1}{ne}\boldsymbol{\nabla}p_e - \mathbf{E}'\cdot\mathbf{B}'\right]d^3x$$

- The reference fields must have the same tangential electric field and total magnetic flux so that the relative helicity evolution is

$$\frac{\partial\mathcal{K}}{\partial t} = \int\left[-\underline{2\left(\mathbf{v}_{\mathrm{eq}}\times\mathbf{B}_{\mathrm{eq}}\right)\cdot\mathbf{B}} - \underline{2\eta\left(\mathbf{J}-\mathbf{J}_{\mathrm{eq}}\right)\cdot\mathbf{B}} + \underline{2\mathbf{B}\cdot\tfrac{1}{ne}\boldsymbol{\nabla}p_e}\right]d^3x$$

The magnetic energy evolution over the crash is dominated by the resistive term.

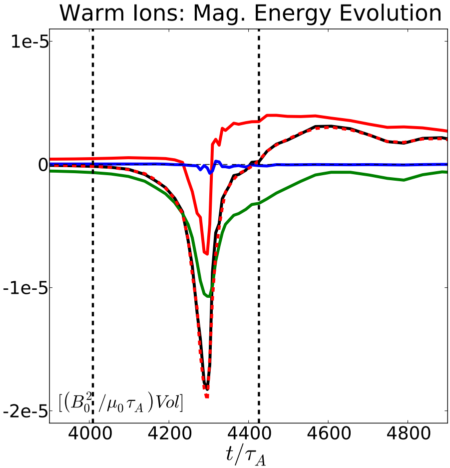

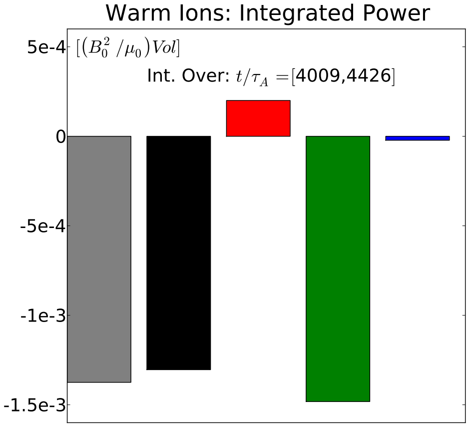

- The dashed red curve shows a finite difference estimate of $\frac{\partial W_B}{\partial t}$

$$\frac{\partial W_B}{\partial t} = \int \left[\underline{(\mathbf{v}\times\mathbf{B} - \mathbf{v}_{eq}\times\mathbf{B}_{eq})\cdot\mathbf{J}} - \underline{\eta\,(\mathbf{J}-\mathbf{J}_{eq})\cdot\mathbf{J}} + \underline{\mathbf{J}\cdot\frac{1}{ne}\boldsymbol{\nabla}p_e} \right] d^3x$$

The electron pressure in magnetic helicity evolution is weak and there is little coupling of $\mathcal{K}$ and $\mathcal{X}$.

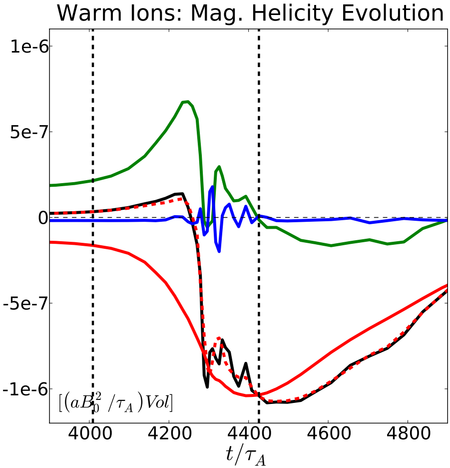

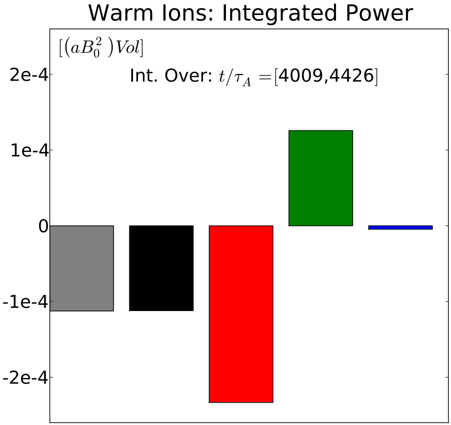

- The dashed red curve shows a finite difference estimate of $\frac{\partial \mathcal{K}}{\partial t}$

$$\frac{\partial \mathcal{K}}{\partial t} = \int \left[-\underline{2\left(\mathbf{v}_{\text{eq}} \times \mathbf{B}_{\text{eq}}\right) \cdot \mathbf{B}} - \underline{2\eta\left(\mathbf{J} - \mathbf{J}_{\text{eq}}\right) \cdot \mathbf{B}} + \underline{2\mathbf{B} \cdot \frac{1}{ne} \boldsymbol{\nabla} p_e} \right] d^3x$$

Including the ion gyroviscosity significantly alters the evolution of the cross helicity at the relaxation event.

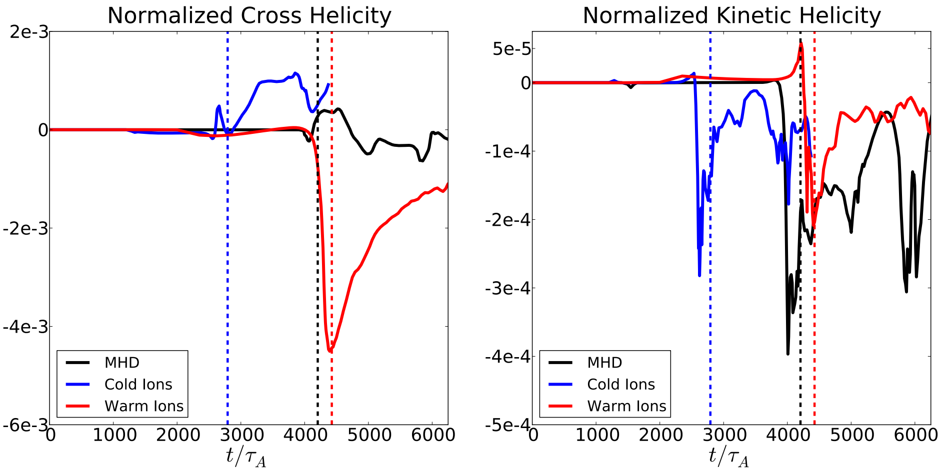

- The cross and kinetic helicities are normalized by the initial value of the magnetic helicity
- The kinetic helicity evolution appears similar for all cases

Cross helicity evolution is dominated by the viscous and gyroviscous pieces in simulations.

- Variational theories that conserve hybrid helicities neglect viscous dissipation and do not account for gyroviscous effects

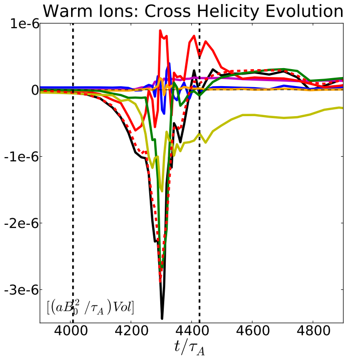

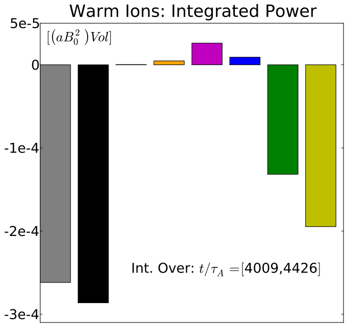

$$2\left(\frac{m_i}{e}\right)\frac{\partial \mathcal{X}}{\partial t} = \int \left[-2\left(\frac{m_i}{e}\right)\left(\frac{1}{ne}\right)(\mathbf{J}\times\mathbf{B})\cdot\nabla\times\mathbf{v} + 2\left(\frac{m_i}{e}\right)\left(\frac{1}{ne}\right)\nabla p_e\cdot\nabla\times\mathbf{v}\right] d^3x$$

$$+\int\left[-2\left(\frac{m_i}{e}\right)\eta\mathbf{J}\cdot\nabla\times\mathbf{v} - 2\mathbf{B}\cdot\left(\frac{1}{ne}\nabla p\right) - \frac{2\mathbf{B}}{ne}\cdot\left(\nabla\cdot\underline{\mathbf{\Pi}}_{iso}\right) - \frac{2\mathbf{B}}{ne}\cdot\left(\nabla\cdot\underline{\mathbf{\Pi}}_{gyr}\right)\right]d^3x$$

The kinetic helicity evolution is under-resolved but has large contributions from viscosity and gyroviscosity.

- The kinetic helicity contribution is small: $\mathcal{H} \sim 10^{-1}\mathcal{X}$ and $\mathcal{H} \sim 10^{-4}\mathcal{K}$

$$H = \left[aB_0^2 Vol\right] \int \left\{ \hat{\mathbf{A}} \cdot \hat{\mathbf{B}} + 2\left(\frac{d_i}{a}\right) \hat{\mathbf{v}} \cdot \hat{\mathbf{B}} + \left(\frac{d_i}{a}\right)^2 \hat{\mathbf{v}} \cdot \left(\hat{\mathbf{\nabla}} \times \hat{\mathbf{v}}\right) \right\} d^3\hat{x}$$

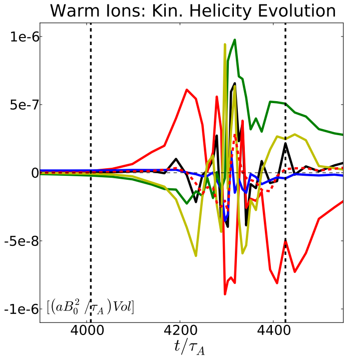

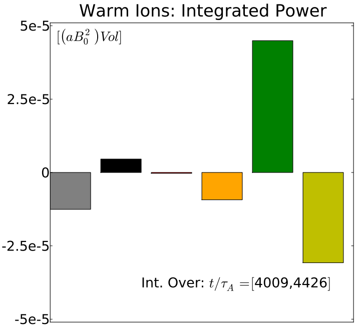

$$\left(\frac{m_i}{e}\right)^2 \frac{\partial \mathcal{H}}{\partial t} = 2\frac{m_i}{e} \int \left[\underline{\mathbf{J} \times \mathbf{B}} - \underline{\mathbf{\nabla} p} - \underline{\mathbf{\nabla} \cdot \mathbf{\Pi}_{iso}} - \underline{\mathbf{\nabla} \cdot \mathbf{\Pi}_{gyr}} \right] \cdot \frac{\mathbf{\nabla} \times \mathbf{v}}{ne} d^3x$$

Outline

Unresolved issue with internal energy evolution.

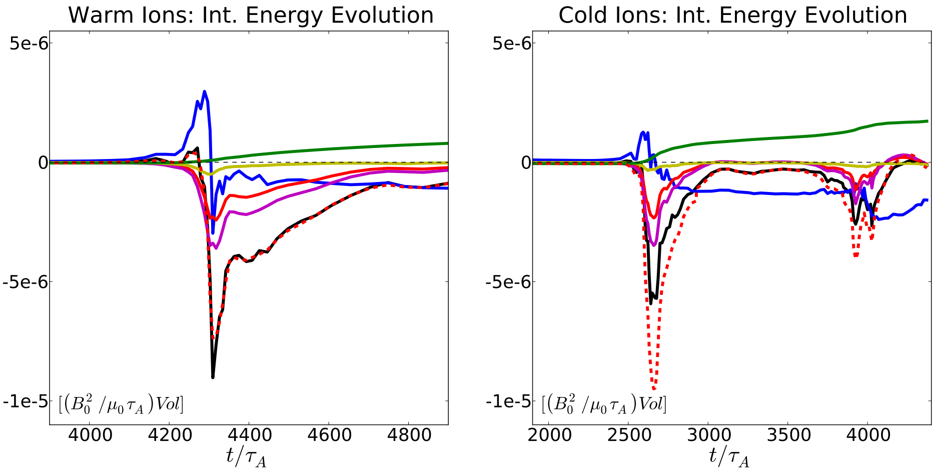

$$\frac{\partial W_p}{\partial t} = \int \left[2\left(\chi n \boldsymbol{\nabla} T\right) + \frac{2T}{\Gamma-1} D_n \boldsymbol{\nabla} n \right] \cdot \hat{\mathbf{n}} dA + \int \left[\mathbf{v}\cdot\boldsymbol{\nabla} p - \frac{2}{\Gamma-1} D_n \boldsymbol{\nabla} n \cdot \boldsymbol{\nabla} T - \frac{2}{\Gamma-1} n_{\text{eq}} \mathbf{v}_{\text{eq}} \cdot \boldsymbol{\nabla} T \right] d^3x$$

This discrepancy is under investigation.

- **All** simulations with ion gyroviscosity (my cases at S=5e3, S=2e4, and Jake's S=8e4 case) accurately capture internal energy evolution
- Cases with MHD Ohm's law and 2-fluid Ohm's law without gyroviscosity show this discrepancy

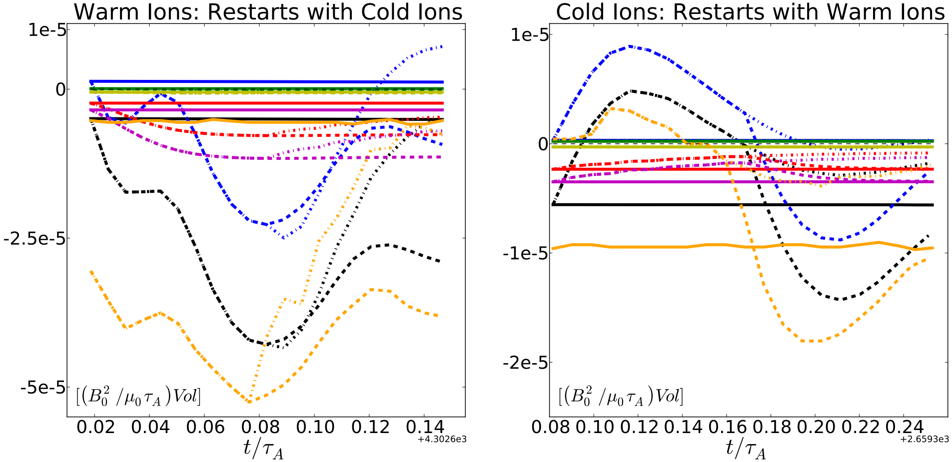

Outline

Conclusions

- Relaxation theories attempt to predict the preferred plasma state by minimize some quantities while conserving others
  - Ideal invariants in a two-fluid model are the energy and the hybrid helicity
  - Minimizing the energy while conserving the hybrid helicity results in an ill-posed mathematical problem (see Ohsaki ref., slide 10)
- Numerical simulations examine the evolution of the ideal invariants within the extended MHD model
  - Magnetic helicity is robustly conserved relative to magnetic energy
  - Cross helicity evolution is dominated by viscosity and gyroviscosity
  - First order FLR effects (ion gyroviscosity) has **not** been included in any relaxation theories but warm ion simulations suggest it is important
- Diagnostics measuring helicity evolution accurately capture the large scale dynamics
  - Kinetic helicity evolution appears under-resolved
  - However, it is the smallest contributor to hybrid helicity
  - To the order of the cross helicity, the evolution is well-resolved